

GA-A23404

TOLERABLE ELMs AT HIGH DENSITY IN DIII-D

by
A.W. LEONARD, T.H. OSBORNE, M.E. FENSTERMACHER,
C.J. LASNIER, and M.A. MAHDAVI

JULY 2000

DISCLAIMER

This report was prepared as an account of work sponsored by an agency of the United States Government. Neither the United States Government nor any agency thereof, nor any of their employees, makes any warranty, express or implied, or assumes any legal liability or responsibility for the accuracy, completeness, or usefulness of any information, apparatus, product, or process disclosed, or represents that its use would not infringe privately owned rights. Reference herein to any specific commercial product, process, or service by trade name, trademark, manufacturer, or otherwise, does not necessarily constitute or imply its endorsement, recommendation, or favoring by the United States Government or any agency thereof. The views and opinions of authors expressed herein do not necessarily state or reflect those of the United States Government or any agency thereof.

TOLERABLE ELMs AT HIGH DENSITY IN DIII-D

by
A.W. LEONARD, T.H. OSBORNE, M.E. FENSTERMACHER,
C.J. LASNIER,* and M.A. MAHDAVI

This is a preprint of a paper presented at the 14th International Conf. on Plasma Surface Interactions in Controlled Fusion Devices, May 22-26, 2000 in Rosenheim, Germany and to be published in *J. Nucl. Mater.*

*Lawrence Livermore National Laboratory, Livermore, California

Work supported by
the U.S. Department of Energy under Contract Nos. DE-AC03-99ER54463,
and W-7405-ENG-48

GA PROJECT 30033
JULY 2000

ABSTRACT

The energy released at each ELM is found to decrease in relation to the pedestal pressure, by more than a factor of five, as the line-averaged density in DIII-D H-mode is raised from about half the Greenwald density limit to near the Greenwald limit. The pedestal pressure remains nearly constant over this range demonstrating an attractive regime for future larger tokamaks. The reduction in ELM energy, in both low and high triangularity configurations, is seen to scale more with the pedestal electron temperature than the pedestal density. At low density both the electron density and temperature inside the separatrix drop due to the ELM instability; however at high density the density perturbation remains similar while the temperature profile is unaffected. ELMs at high density are also characterized by smaller magnetic fluctuations consistent with a higher toroidal mode number ELM instability.

1. INTRODUCTION

Edge-Localized-Modes (ELMs) remain a serious concern for future large tokamaks. The ELM instability relieves the plasma pressure gradient that builds just inside the separatrix and releases energy and particles into the Scrape-Off-Layer (SOL) in a very short time, < 1 ms [1,2]. The very large transient heat flux due to individual ELMs can lead to divertor surface ablation and unacceptable target plate erosion [3]. A previous multi-machine study [4] of low to moderate density H-mode found that the energy released at each ELM was approximately 1/3 of the pedestal electron energy. The pedestal energy is defined as the pedestal pressure times the plasma volume. The conclusion of this result was somewhat discouraging in that high pedestal values desired for good confinement in future large tokamaks could lead to unacceptable divertor target erosion.

In this paper we extend the previous work to examine ELM behavior at higher density. This effort is concerned with Type I ELMs where the edge pedestal is large. Other small ELM regimes [5], such as Type III, typically have a smaller edge pedestal and lower confinement. While the previous study examined Type I ELMs at about half of the Greenwald density, future tokamaks are expected to operate at close to the Greenwald density to maximize fusion power output, and it is important to determine ELM behavior in this more relevant higher density regime. The Greenwald density, n_{GW} , is a commonly observed density limit in tokamaks and is defined as $n_{GW}(m^{-3}) = 10^{14} I_p/\pi a^2$ where I_p (amps) is the plasma current and a (meters) is the plasma minor radius. We find that as density increases the energy lost at each ELM becomes much smaller in relation to the pedestal pressure. These ELMs are small enough that future tokamaks could operate with a large pedestal in this regime and still not threaten the divertor target due to ELM heat flux. A description of the experimental setup is described in the next section. The scaling of ELM energy and other characteristics with increasing density is presented in Section 3. Finally a discussion of the results and remaining work for scaling to larger tokamaks is given in Section 4.

2. EXPERIMENTAL SETUP AND DIAGNOSTICS

For these experiments neutral deuterium gas puffing is used to vary the plasma density in H-mode while keeping other parameters fixed, primarily the plasma current of 1.2 MA and toroidal field of 2.0 T. These Lower-Single-Null (LSN) discharges are in a low triangularity private flux pumping configuration. With gas puffing the divertor pumping produces steady-state operation more quickly allowing for a longer evaluation of ELM behavior without discharge evolution. This divertor configuration is also found to more robustly allow high density operation without reverting to L-mode. Two cases are studied, a low upper triangularity case of $\delta \sim 0.0$, Fig. 1(a), and a higher triangularity case of $\delta \sim 0.36$, Fig. 1(b). The higher triangularity and its associated higher stability limit is used to separate variations of pedestal density and temperature.

Two of the low triangularity discharges at different densities are shown in Fig. 2. By increasing the gas puffing the line-averaged density increases by approximately a factor of two. At the same time the pedestal density increases by a similar amount indicating the density profile

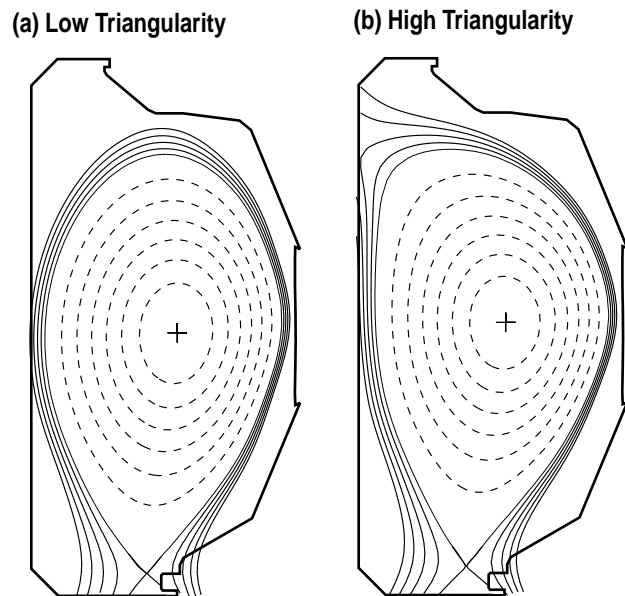


Fig. 1. The magnetic configurations used for these experiments. The divertor geometry is optimized for pumping of the private flux region. The lower half triangularity is constant at $\delta \sim 0.1$, while the upper triangularity is changed between (a) at $\delta = 0.0$ and (b) $\delta = 0.36$.

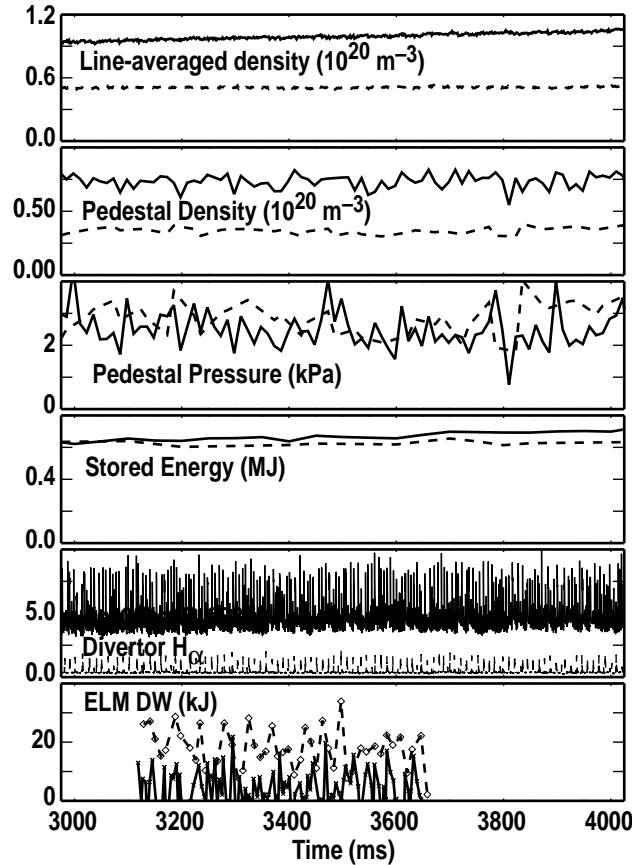


Fig. 2. The time behavior of a typical discharge with and without gas puffing. The high density data is represented by the solid line, the low density data by the dashed line. Shown are the line-averaged and pedestal densities, the pedestal pressure, plasma stored energy and divertor H_{α} . The energy lost at each ELM is determined from equilibrium calculations from fast magnetic measurements which have a limited acquisition window.

peaking is not significantly changed. The pedestal pressure and plasma stored energy, however, remain nearly constant. Maintaining good confinement with a robust pedestal is consistent with a stiff temperature profile keeping the central electron temperature proportional to the pedestal electron temperature as the overall density increases.

The ELM character changes significantly at high density with rapid ELMs, as seen in the H_{α} signal, and a smaller energy lost at each ELM, Fig. 2. The energy lost at each ELM is measured by fast magnetic equilibrium analysis. The plasma stored energy is calculated every 0.5 ms in a selected time window for fast magnetic data acquisition. The ELM energy is determined by evaluating the difference in the plasma energy within 1.5 ms before and after each ELM, with a

fast rise in the divertor H_{α} signal indicating the time of each ELM. The noise and uncertainty in this measurement is typically about 5 kJ for each ELM.

The edge electron temperature, density and pressure profiles both before and after an ELM for both low and high density are shown in Fig. 3. The edge profiles are measured with a Thomson scattering system collecting a profile every 12 ms. The pre-ELM profiles are gathered by collecting all the Thomson data, within a steady-state data window, that falls within 1.5 ms before the onset of the ELM instability. The Thomson data is then mapped to the mid-plane. The pedestal values, $n_{e,ped}$, $T_{e,ped}$, and $P_{e,ped}$, are then determined by fitting the collected profiles to a \tanh function in the edge and a linear profile inside the steep gradient region. The post-ELM profiles are collected in a similar data window, but after an ELM.

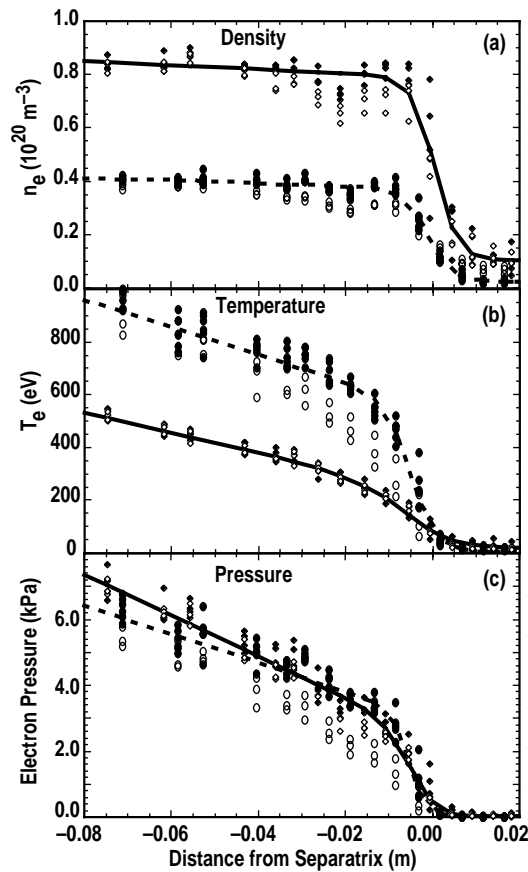


Fig. 3. Edge profiles collected within 1.5 ms before (closed symbols) and 1.5 ms after (open symbols) an ELM from Thomson scattering. The profiles are fitted with a \tanh function to determine the pedestal values. Shown are the (a) density, (b) electron temperature, (c) the electron pressure. The diamond symbols and solid \tanh fitting line are for high density. The dashed line and circular symbols represent low density.

3. EXPERIMENTAL RESULTS

Though the ELM energy decreases at higher density, as shown by the example in Fig. 2, the relationship of ELM energy to pedestal pressure is the important aspect under study in this paper. Future tokamaks will require both a large edge pedestal pressure for confinement and small ELMs to protect the divertor. A previous study [6] of the pedestal and confinement in this configuration showed the pedestal pressure remained relatively constant up to a density of $n_{e,ped} \sim 70\% - 75\%$ of n_{GW} . This corresponds to a line-averaged density of about 95% of n_{GW} for both low and high triangularity discharges. The high triangularity configuration with its increased ideal edge stability nearly a factor of two higher pedestal pressure below the degradation threshold. In terms of the pedestal temperature, $T_{e,ped}$, the pedestal begins to degrade at $T_{e,ped} \sim 300$ eV for low triangularity and $T_{e,ped} \sim 500$ eV at high triangularity.

As density is raised the ELM energy becomes smaller in relation to the edge pressure pedestal. This reduction is summarized in Fig. 4(a) where the ELM energy ratio decreases with increasing pedestal density. In Fig. 4 ΔW_n is defined as the energy lost at each ELM divided by the pedestal electron energy, or $P_{e,ped}$, times the plasma volume. As $n_{e,ped}$ increases ΔW_n decreases continuously until the ELM size is within the measurement uncertainty. Also shown in Fig. 4 is the value of ΔW_n that was previously obtained from the multi-machine scaling at a density of $\sim 40\%$ of n_{GW} . As the pedestal pressure is constant up to $n_{e,ped} \sim 70\%$ n_{GW} any reduction in the ΔW_n below $n_{e,ped} \sim 70\%$ n_{GW} represents an absolute reduction in ELM size. The parameters at the pedestal degradation threshold then represent an attractive regime for future tokamaks with a robust pedestal, tolerable ELMs and line-averaged density very near n_{GW} .

The value of ΔW_n at a given $n_{e,ped}$ varies considerably from the low to the high triangularity configuration. The density is apparently not the sole determining factor for ELM size. In Fig. 5(b), the same ELM data is plotted versus the pedestal electron temperature, $T_{e,ped}$. Now the data from the low and high triangularity cases lie along the same curve. This data indicates that

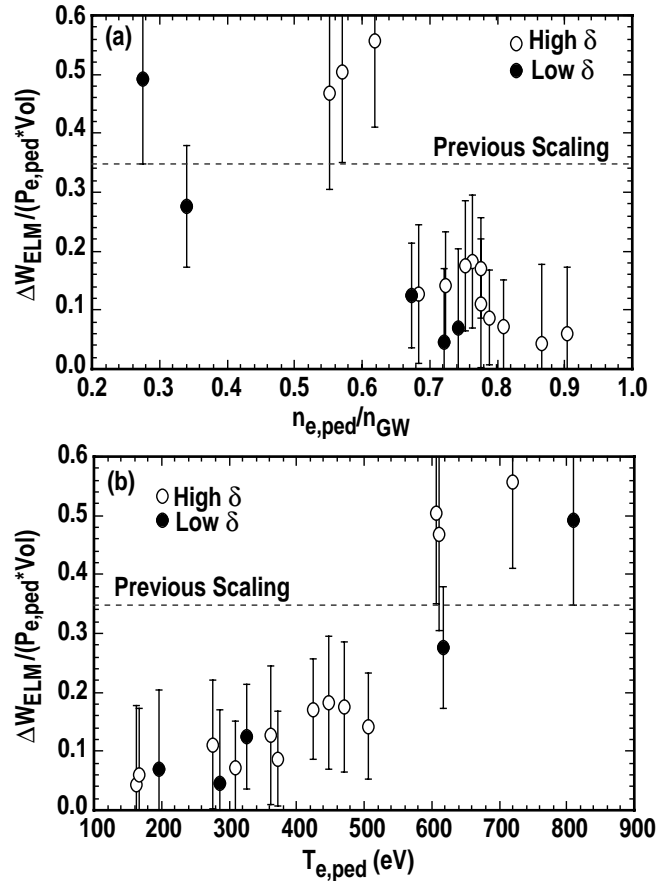


Fig 4. ΔW_n , the ELM energy normalized by the pedestal electron energy, plotted as a function of (a) the pedestal density, and (b) the pedestal electron temperature.

$T_{e,ped}$, or some process more closely associated with temperature, is more critical in controlling the amplitude of the ELM instability.

In order to gain insight into the mechanisms controlling the ELM size it is useful to examine details of the ELM itself more closely. A few of the details of the ELM instability for the low triangularity case can be seen, Fig. 3, in the edge electron density, temperature, and pressure profiles just before and after an ELM. The closed symbols are profiles collected from the DIII-D Thomson scattering system less than 1.5 ms before an individual ELM, with the closed symbols representing profiles less than 1.5 ms after an ELM. The solid lines are *tanh* fits through the pre-ELM profiles at high density while the dashed lines are fits through low density profiles. At low density the ELM perturbs the density profile far inside the separatrix. The density drops quickly

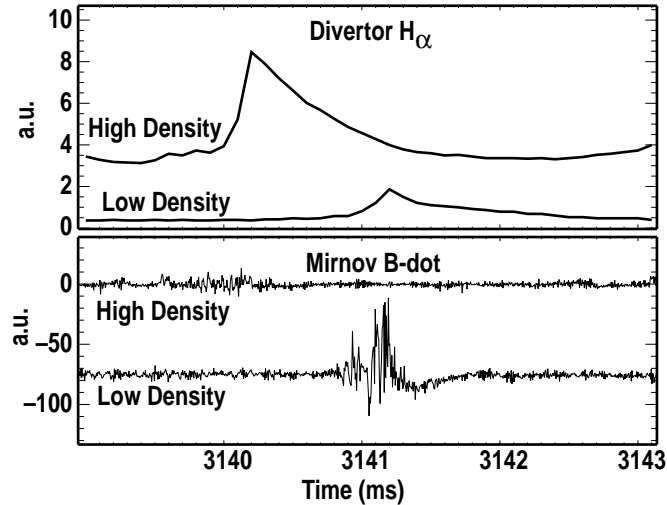


Fig 5. The low and high density behavior of an individual ELM on an expanded time scale as evidenced by (a) H_{α} emission in the divertor and (b) magnetic fluctuations measured by a Mirnov B-dot probe.

by 20%–30% to about 4 cm inside the separatrix at the midplane. At high density the pedestal density drops at the ELM a similar amount, but the perturbation does not extend as far inside the separatrix, only 2–3 cm. The differences between high and low density ELMs show up particularly in perturbations to the T_e profile, as shown in Fig. 3(b). The T_e profile at low density is significantly perturbed by the ELM far inside the separatrix. However at high density almost no change can be observed in the T_e profile before and after an ELM. These profiles are combined in Fig. 3(c) to plot the ELM perturbation to the pressure profile, which should be directly related to the ELM energy loss. At low density the ELM causes a drop in $P_{e,ped}$ by up to a factor of 2. This perturbation extends inside the pedestal up to about 5 cm inside the separatrix. At high density, however, the ELM perturbation to the pressure is much more modest and only extends inside the separatrix slightly past the pedestal. Summarizing, it appears that at low density the ELM transports significant energy and particles from far inside the separatrix, and pedestal, across the separatrix into the scrape-off-layer. However at high density only density is carried across the separatrix due the ELM, and the perturbation is limited to near the pedestal region.

There are other changes to the ELM instability that can be observed as the density increases. Plotted in Fig. 5 are divertor H_{α} and magnetic fluctuation signals for individual ELMs at both

high and low density. The time scale has been greatly expanded to highlight the behavior of a single ELM. The baseline divertor H_{α} level is higher in the higher density case, as might be expected from higher recycling levels. At the ELM onset the H_{α} signal rises to a greater level in the high density case compared to low density even though, as shown previously, the energy transported by the ELM is smaller at high density. This comparison points out that increases in H_{α} signals are not a good measure of the ELM energy as H_{α} is related more to edge plasma and neutral density than it is to energy transport or power.

The magnetic fluctuation level also displays distinct differences between low and high density. The magnetic signals are obtained from Mirnov B-dot probes in the divertor. At low density the magnetic fluctuations increase at the start of the rise in H_{α} , and quickly grow reaching a peak at the same time as the peak in the H_{α} signal. The ELM instability then quickly shuts off resulting in a rapid drop in the magnetic fluctuation level and a slower drop in the H_{α} level. The slower decay of the H_{α} signal is due the slower neutral particle transport time in the divertor. For the high density case the magnetic fluctuations during the ELM are smaller, by a factor of 8 to 10, than for low density. In fact the fluctuations rise only slightly above the background noise level. The duration of the fluctuations is $\sim 300 \mu\text{s}$ in all cases.

The reduction in magnetic fluctuation level can arise from two effects. First the ELM instability may saturate at a lower level at high density. A lower instability level should lead to a smaller magnetic fluctuation signal and a slower rate of cross field transport. This would result in a lower ELM energy at higher density if the ELM instability duration does not change. Another possibility is a change in the mode structure itself. Because the magnetic probes are located away from the magnetic surface of the ELM instability the magnetic fluctuation level will fall off as r^{-m} where m is the mode number of the ELM instability. If at high density the mode number of the instability increases, the radial extent of the perturbation will be smaller leading to lesser transport. This reduced ELM energy may occur even though the fluctuation level at the resonant surface is the same as the low density case. In our case both the instability amplitude and mode number may be playing a role in reducing the ELM energy loss at high density.

4. DISCUSSION

In order to scale the ELM energy loss to future large tokamaks a model is needed that incorporates the physical mechanism controlling the ELM amplitude. It is unlikely that n_e or T_e alone is controlling the ELM instability, but parameters such as collisionality, resistivity and neutral flux may be important. Also the large variability in individual ELMs will make it very difficult to determine an ELM scaling from the present results without a physical model as a guide. Following is a discussion of several physical mechanisms that could possibly affect the ELM instability. Further work will be required to determine the importance of these effects.

A common model for increased transport during an ELM is that magnetic instabilities grow until modes overlap producing a stochastic magnetic topology in the high gradient region. Parallel transport would then allow a high flux of energy across the separatrix into the SOL. Since parallel heat conduction is such a strong function of electron temperature, $T_e^{7/2}$, rapid energy transport would cause a quick drop in electron temperature significantly inside the separatrix. This may be the type of transport that is responsible for the drop in T_e as seen in the low density case. Another possibility for transport is that growing instabilities eventually leads to magnetic reconnection carrying plasma across the separatrix. This convective transport would likely not perturb the electron temperature as much as conductive transport. The high density ELMs may be a transition from conductive to convective transport. In order to study and understand the ELM transport a better model of the instability itself is needed.

One model of edge stability in H-mode [7] utilizes the large edge bootstrap current due to the steep pressure gradient of the H-mode barrier. The bootstrap current reduces the magnetic shear in the pedestal and stabilizes the higher order pressure driven ballooning modes. The pressure gradient may then rise until lower mode number current/pressure driven modes become unstable. The lower order modes may be more virulent and produce a bigger perturbation because they can grow to larger amplitude before saturation and island overlap. Also the mode penetrates further inside the plasma because the magnetic perturbation does not drop off as rapidly as the higher

order modes. As density increases the resulting higher collisionality reduces the edge bootstrap current. This might lead to destabilization of higher order pressure driven modes at a lower pressure gradient than the lower order modes. The level of reduced pressure gradient at higher order mode onset must still be determined by further modeling.

There are other effects which might also be playing a role in the scaling of ELM amplitude. Increasing resistivity with a lower electron temperature could slow the growth rate of the modes. Another factor could be neutral fueling in the pedestal region. These and other effects need to be investigated before a definitive scaling can be determined.

5. SUMMARY

We have shown that as density increases in DIII-D the ELMs of H-mode become much more rapid and of smaller amplitude. The energy transported across the separatrix by individual ELMs at high density are more than 5 times smaller than the previous multi-machine scaling at lower density. If the ELMs of future large tokamaks are also 5 times smaller than the low density scaling then future divertor targets should tolerate the associated heat pulses, while maintaining a robust pedestal. However, it is not yet possible to accurately scale these optimistic results to larger tokamaks until the underlying mechanisms are identified. This might be accomplished by comparison of experimental results with modeling and theory and further multi-machine experimental comparisons.

REFERENCES

- [1] P. Gohil, M.A. Mahdavi, L.L. Lao, *et al.*, Phys. Rev. Lett. **61** (1989) 1603.
- [2] H. Zohm, T.H. Osborne, K.H. Burrell, *et al.*, Nucl. Fusion **35** (1995) 543.
- [3] H.D. Pacher, “E9. Disruption and ELM Erosion,” Appendix E9, Section 1.7 (Divertor), ITER Design Description Document, ITER No. “G 17 DDD 1 96-08-21 W2.1,” August 1996.
- [4] A.W. Leonard, A. Herrmann, K. Itami, *et al.*, J. Nucl. Mater. **266-269** (1999) 109.
- [5] H. Zohm, Plasma Phys. Control. Fusion **38** (1996) 105.
- [6] T.H. Osborne, J.R. Ferron, M.E. Fenstermacher, *et al.*, “The Effect of Plasma Shape on H-mode Pedestal Characteristics,” accepted for publication in Plasma Phys. And Contr. Fusion.
- [7] J.R. Ferron, M.S. Chu, G.L Jackson, “Modifications of H-mode Pedestal Instabilities in the DIII-D Tokamak,” accepted for publication in Phys. of Plasmas.

ACKNOWLEDGMENT

Work supported by U.S. Department of Energy under Contracts DE-AC03-99ER54463 and W-7405-ENG-48.